



Increased fibroblast density in actinic cheilitis: association with tryptase-positive mast cells, actinic elastosis and epithelial p53 and COX-2 expression

Isolde G. Rojas¹, Yadira V. Boza^{1,2,3}, Maria Loreto Spencer⁴, Maritza Flores⁵, Alejandra Martínez⁴

¹Department of Oral Surgery & Laboratory of Oral Biology and Pathology, College of Dentistry, University of Concepción, Concepción, Chile; ²Dental Science MS Program, Graduate School, College of Dentistry, University of Chile, Santiago, Chile; ³College of Dentistry, University of Costa Rica, San José, Costa Rica; ⁴Department of Oral Pathology, College of Dentistry, University of Concepción, Concepción, Chile; ⁵Department of Public Health, College of Medicine, University of Concepción, Concepción, Chile

BACKGROUND: Actinic cheilitis (AC) is characterized by epithelial and connective tissue alterations caused by ultraviolet sunlight overexposure known as photodamage. Fibroblasts have been linked to photodamage and tumor progression during skin carcinogenesis; however, their role in early lip carcinogenesis remains unknown. The aim of this study was to assess the density of fibroblasts in AC and normal lip (NL) samples and determine their association with markers of lip photodamage.

METHODS: Fibroblasts, mast cells, p53, COX-2, and elastin were detected in NL ($n = 20$) and AC ($n = 28$) biopsies using immunohistochemistry/histochemistry. Mast cell and fibroblast density and epithelial p53 and COX-2 expression scores were then obtained. Elastosis was scored 1–4 according to elastin fiber density and tortuosity.

RESULTS: Fibroblasts, mast cells, p53, COX-2, and elastosis were increased in AC as compared to NL ($P < 0.001$). Multivariate analysis showed an association between fibroblast and mast cell density at the papillary and reticular areas of AC and NL ($P < 0.05$). Papillary fibroblast density was also associated with epithelial p53 and COX-2 expression ($P < 0.05$). Increased fibroblast density, both papillary and reticular, was found in the high elastosis group (scores 3–4) as compared to the low elastosis group (scores 1–2) ($P < 0.01$). Increased reticular mast cell density was detected only in the high elastosis group ($P < 0.01$).

CONCLUSIONS: Fibroblasts are increased in AC, and they are associated with mast cell density, epithelial p53 and COX-2 expression, and actinic elastosis. Therefore, fibroblasts may contribute to lip photodamage and could be considered useful markers of early lip carcinogenesis.

J Oral Pathol Med (2012) 41: 27–33

Keywords: actinic cheilitis; actinic elastosis; COX-2; fibroblasts; mast cells; p53; photodamage

Introduction

Actinic cheilitis (AC) is a potentially malignant disorder of the lip vermilion characterized by epithelial and connective tissue alterations induced mainly by overexposure to ultraviolet (UV) sunlight, a process known as photodamage (1–3). Epithelial alterations of AC include an increased expression of proapoptotic and proinflammatory markers such as p53 and cyclooxygenase (COX)-2 (4–6). Connective tissue changes are characterized by increased immune cell infiltration, e.g., mast cells and lymphocytes (7–9), and by actinic elastosis, a prominent feature of photodamaged tissues (2, 9).

Elastosis frequently begins at the junction of the papillary and reticular areas of the dermis (10). It is characterized by the accumulation of tangled masses of dystrophic elastic fibers, disorganized tropoelastin and fibrillin, increased amounts of ground substance, and collagen degradation (11). Mast cells and fibroblasts have been associated with elastosis formation in photodamaged skin (11–15). It has been postulated that mast cells stimulate elastosis by the production of proteases, such as tryptase and matrix metalloproteinase (MMP)-9, and by the activation of fibroblasts to secrete elastin (12, 13). Nevertheless, the role of mast cells in elastosis formation has been controversial, because some studies have not found a correlation between mast cell density and increased elastin content either in photodamaged skin or in the lips (9, 16). On the other hand, fibroblasts, the most abundant resident cells of skin and mucosae (17) whose main function is to maintain extracellular matrix (ECM) homeostasis, stimulate elastosis formation by different mechanisms. While both increased elastin

synthesis and degradation by fibroblasts contribute to dystrophic elastic fiber accumulation (14, 18, 19), their role in the pathogenesis of actinic elastosis in the lip has not been determined.

Fibroblast density and activation are increased in physiological responses, such as wound healing, and in disease states, such as fibrotic disorders and carcinogenesis (20–23). During epithelial carcinogenesis, fibroblasts have paracrine and autocrine interactions with resident and immune cells that include keratinocytes and mast cells (17, 24, 25). While fibroblasts can stimulate keratinocyte migration, proliferation, and malignant transformation (26, 27), mast cells and transformed epithelial cells stimulate fibroblasts to acquire an activated phenotype that favors tumor progression (13, 27–30).

Therefore, it was hypothesized that epithelial and connective tissue alterations of AC lesions are associated with increased fibroblast density. To test this hypothesis, fibroblasts and mast cells were detected using double immunohistochemistry in normal lip and AC samples. In addition, mast cell density, actinic elastosis, and epithelial p53 and COX-2 expression were analyzed to determine the associations between fibroblast density and markers of lip photodamage.

Material and methods

Patients and lip tissues

A total of 48 human biopsies of lower lip vermilion classified as normal lip ($n = 20$, age 41 ± 13 , 43% males) and AC ($n = 28$, age 51 ± 13 , 66% males) were retrieved from the Archives of the Oral Biology and Pathology Laboratory, School of Dentistry, University of Concepción. Informed consent was obtained from all subjects, and this study was approved by the Ethics Committee of the University of Concepción. Samples were fixed in 10% buffered formalin (pH 7.4) and paraffin-embedded within 24 h. Serial sections, 4 μ m thick, were obtained from the tissue blocks and processed for histopathological and immunohistochemical analysis.

Double immunohistochemistry for detection of fibroblasts and mast cells

To simultaneously detect fibroblasts and mast cells in the same tissue section, a double immunohistochemistry technique using primary antibodies of the same species was adapted from Shütz et al. (31). Primary antibody specifications and reaction conditions are listed in Table 1. Briefly, sections were dewaxed, rehydrated, and blocked for endogenous peroxidase and non-specific protein binding. Mast cells were stained first using the

monoclonal mouse anti-tryptase antibody and then by goat anti-mouse IgG-poly-HRP (Chemicon International, Temecula, CA, USA). The reaction was developed with 3-3'-diaminobenzidine (DAB) (Chemicon International). Antigen retrieval was subsequently performed, and fibroblasts were detected using the primary monoclonal antibody mouse anti-prolyl-4-hydroxylase, followed by goat anti-mouse IgG-poly-HRP (Chemicon International) and Vector SG (Vector Labs, Burlingame, CA, USA) as the chromogen. Slides then were counterstained with Fast Red (Vector Labs), dehydrated and mounted. Cervix cancer sections were used as positive controls and incubation with a non-specific mouse antibody of the same isotype (Chemicon International) was used as a negative control for each marker.

Mast cells (brown stain) and fibroblasts (blue stain) were counted in immunostained sections of both normal lip and AC samples by two calibrated observers using an Olympus C31 Microscope (Center Valley, PA, USA) in 10 counting fields ($40\times$ magnification, 0.2 mm^2) at the reticular and papillar areas of each section (total number of counting fields = 20). Results were expressed as cell number/ mm^2 (mean \pm SEM).

Single immunohistochemistry and scoring

Immunohistochemical studies were performed to evaluate epithelial expression of COX-2 and p53. Primary antibody specifications and reaction conditions are listed in Table 1. Briefly, samples were dewaxed, rehydrated, and pretreated for antigen retrieval. Endogenous peroxidase and non-specific protein binding were then blocked, and slides were incubated with the primary antibodies. Immunocomplexes were detected with the Goat Immunocruz Staining System (Santa Cruz Biotechnology, Inc., Santa Cruz, CA, USA) for COX-2 and goat anti-mouse IgG-poly-HRP (Chemicon International) for p53. Slides then were counterstained with Harris Hematoxylin. Positive controls consisted of sections of skin SCC for p53 and colon cancer for the other markers. Negative control for p53 was performed by substituting the primary antibody with its respective isotype. In the case of COX-2, negative controls were performed by replacing it with normal goat serum or with the primary antibody previously incubated for 1 h with COX-2 blocking peptide (Santa Cruz Biotechnology, Inc.) as previously described (6).

For p53 and COX-2 expression analyses, samples were photographed with a Nikon microscope Eclipse 50i connected to a Nikon digital camera DS-5M with Nis-elements 2.2 imaging software (Nikon Instruments, Inc., Melville, NY, USA). A score of epithelial p53 and

Table 1 Primary antibodies (source and clone specification), antigen retrieval, dilution, and incubation time used in immunohistochemistry

<i>Antibody</i>	<i>Antigen retrieval</i>	<i>Dilution/incubation</i>
Tryptase (clone G3; Chemicon International)	None	1:2000/1 h RT
Prolyl-4-hydroxylase (clone 5B5; Dako, Carpinteria, CA, USA)	EDTA pH = 8.0 (1 mM)	1:200/1 h RT
p53 (Clone DO7; Dako)	Citric-acid buffer (10 nM, pH 6.0)	1:100/1 h RT
COX-2 (C-20; Santa Cruz Biotechnology, Inc.)	Citric-acid buffer (10 nM, pH 6.0)	1:400/overnight 4°C

COX-2 expression was subsequently obtained for each sample by two calibrated observers, including extension (percentage of positive cells/field) and intensity (0 = undetectable, 1 = weak, 2 = medium, 3 = strong) of the staining, as previously described (6).

Verhoeff stain of elastic fibers and scoring

As a histological marker of lip photodamage at the lamina propria, elastic fibers were detected using Verhoeff stain. The Van Gieson stain was used as a

counterstainer. The number and diameter of elastic fibers were assessed by two independent examiners using an Olympus C31 Microscope, and a histological scoring of elastosis was determined (1+ to 4+) as described by Grimbaldeston et al. (12). The lowest score 1+ corresponded to a fine meshwork of normal elastin fibers; 2+ corresponded to a mild increase in density and individual thickness of the elastin fibers; 3+ represented a marked increase in elastin fiber density and thickness; and 4+ represented a very marked increase in fiber

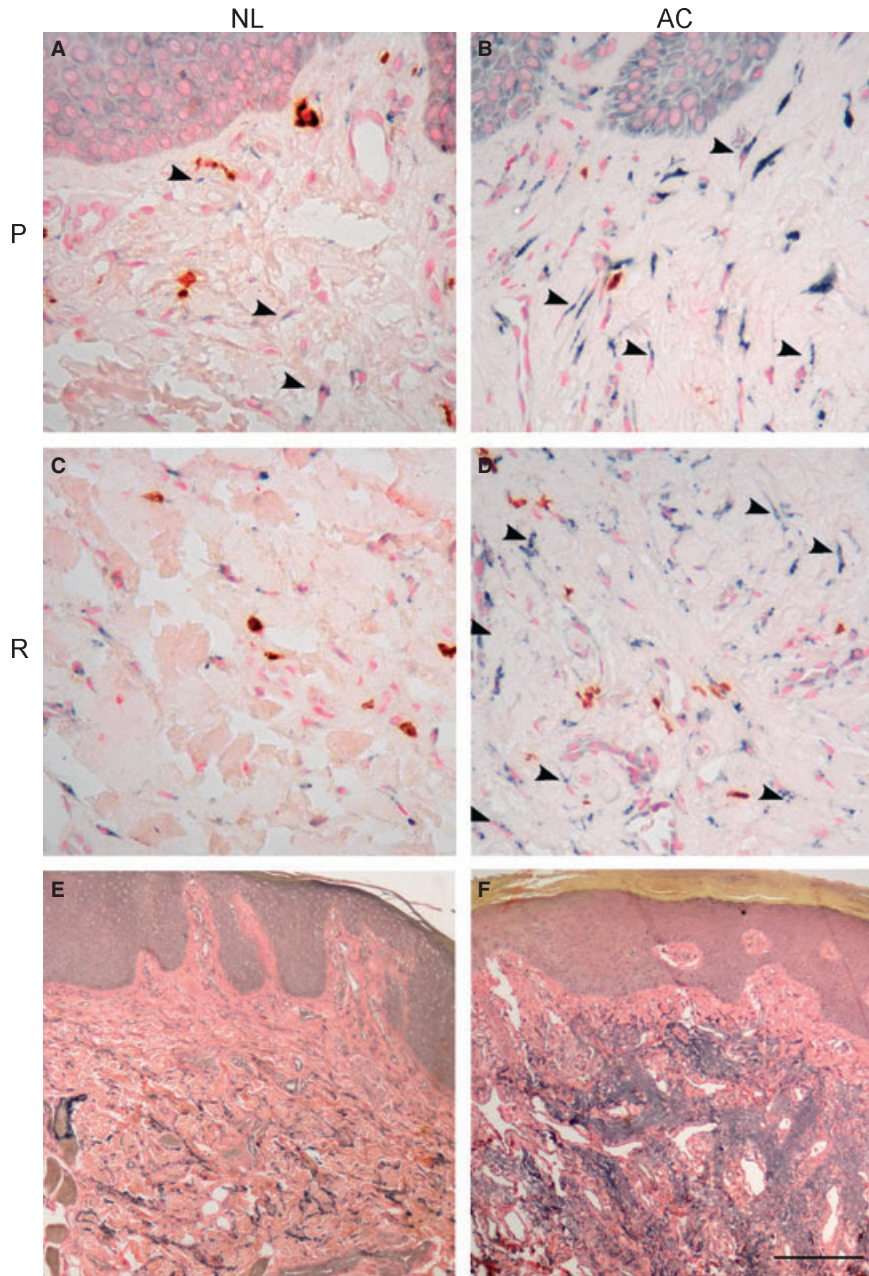


Figure 1 Detection of fibroblasts, mast cells, and elastosis in normal lip (NL) and actinic cheilitis (AC) samples. (A–D) Representative microphotographs of papillary (P) and reticular (R) areas of NL (A and C) and AC (B and D) sections processed for the detection of prolyl-4-hydroxylase-positive fibroblasts (blue stain) and tryptase-positive mast cells (brown stain) by double immunohistochemistry. (E, F) Detection of elastin (purple) and collagen (pink) fibers in NL (E) and AC (F) by Verhoeff-Van Gieson stain. Black arrows indicate prolyl-4-hydroxylase-positive fibroblasts. Bar represents 50 μ m for panels A–D and 100 μ m for panels E–F.

density and thickness with at least focal confluence. In addition, a dichotomic analysis was performed, with a low grade of elastosis corresponding to scores 1 and 2 and a high grade of elastosis corresponding to scores 3 and 4 as described by Costa et al. (9).

Statistical analyses

Statistical tests were performed using SPSS Program 14.0 (Chicago, IL, USA). Data were normally distributed according to the Kolmogorov–Smirnov test, and differences between groups were examined using *t*-test. Qualitative data were analyzed with Fisher’s exact test. Association between variables was determined using multivariate analysis. Differences were considered statistically significant when *P* < 0.05 (two-tailed).

Results

Determination of fibroblasts, mast cells, and markers of lip photodamage

Fibroblasts and mast cells were analyzed using double immunohistochemistry in the lamina propria of normal lip and AC sections. Figure 1(A–D) shows representative microphotographs of fibroblast (blue stain) and mast cell (brown stain) distribution in the papillary and reticular areas of normal lip and AC samples. Actinic elastosis, as detected by Verhoeff–Van Gieson stain, also is shown for normal lip and AC (Fig. 1E,F). Statistical analyses of the results showed an increase in fibroblast and mast cell density in AC as compared to normal lip, both in the papillary and reticular areas of the lamina propria (*P* < 0.0001, *t*-test) (Fig. 2). Actinic elastosis scores were elevated in AC as compared to normal lip (*P* < 0.0001, Fisher’s Exact test) (Table 2), with 82% of the AC samples with high elastosis scores (3–4). Although most of the normal lip biopsies had low elastosis scores (1–2), six of 20 samples had high elastosis scores, with a maximum score of 3. Normal lip and AC samples with high elastosis corresponded to older subjects (*P* < 0.05, Table 2).

As previously described (4, 6), the epithelial markers of lip photodamage, p53 and COX-2, were higher in AC as compared to normal lip (*P* < 0.0001, Mann–Whitney) (Table 2).

Association between fibroblasts, mast cells, and epithelial p53 and COX-2 expression

Using multivariate analyses, a significant association between fibroblast and mast cell density was detected in the papillary (*P* < 0.05) and reticular areas (*P* < 0.0001) of AC and normal lip samples (Table 3). Only papillary fibroblast density was significantly associated with epithelial expression of p53 and COX-2 in AC and normal lip samples (*P* < 0.05) (Table 3).

Association between actinic elastosis and the density of fibroblasts and mast cells

According to the dichotomic elastosis index, AC and normal lip samples were distributed into high (3–4) and low (1–2) elastosis groups. Increased fibroblast density was found in the papillary and reticular areas of the high

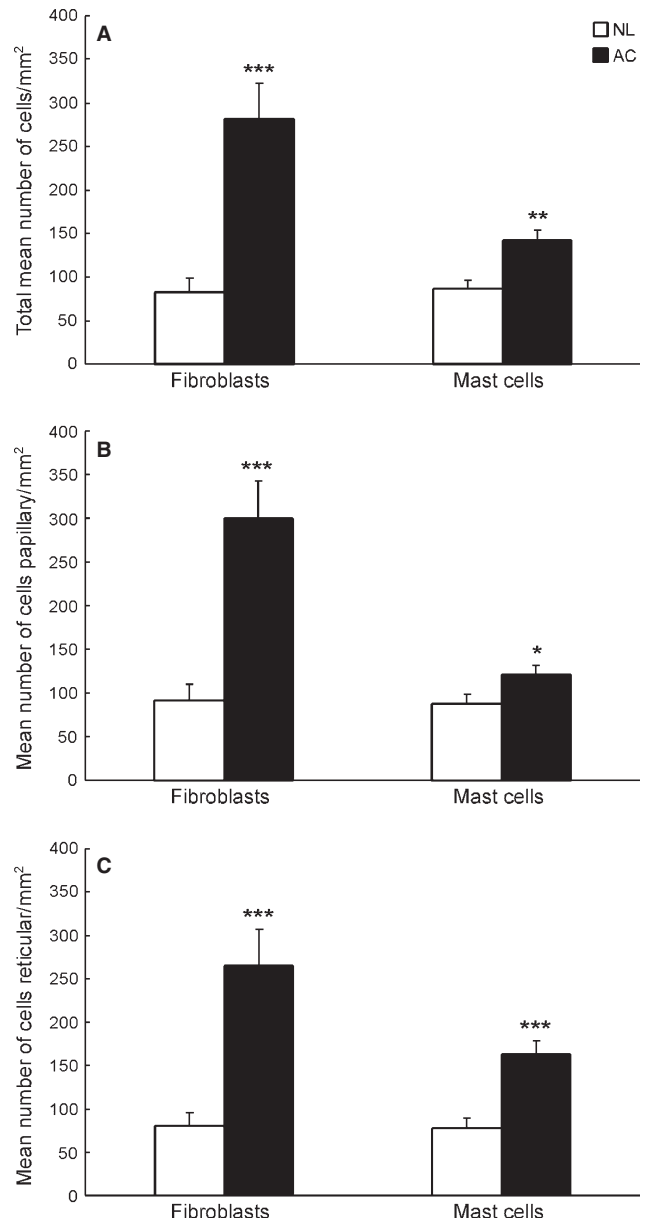


Figure 2 Density of fibroblasts and mast cells in normal lip (NL) and actinic cheilitis (AC). Samples processed for the detection of fibroblasts and mast cells by double immunohistochemistry were analyzed. The number of cells/mm² was determined in total (A), papillary (B), and reticular (C) areas of each sample. Results are expressed as Mean ± SEM. ****P* < 0.0001 (*t*-test) for total, papillary, and reticular fibroblasts and for reticular mast cells in AC as compared to NL. ***P* < 0.001 for total mast cells in AC as compared to NL. **P* < 0.05 for papillary mast cells in AC as compared to NL.

elastosis group as compared to the low elastosis group (*P* < 0.01, *t*-test) (Fig. 3A). Mast cells were increased only in the reticular area of the high elastosis group (*P* < 0.05), with no differences in papillary mast cell density of high and low elastosis groups (Fig. 3B).

Discussion

The results showed that fibroblasts were increased significantly in photodamaged lips in both the papillary

Table 2 Actinic elastosis and epithelial p53 and COX-2 scores in actinic cheilitis (AC) and normal lip samples

	Normal lip (n = 20)	AC (n = 28)	P-value
Elastosis score			
Low 1–2, [age, years]	14 (70%), [37 ± 13]	5 (18%), [38 ± 18]	$P < 0.001^b$
High 3–4, [age, years]	6 (30%), [52 ± 5] [$P < 0.05^a$]	23 (82%), [54 ± 11] [$P < 0.05^a$]	$P < 0.001^b$
p53 score (mean ± SEM)	25 ± 6	95 ± 11	$P < 0.0001^c$
COX-2 score (mean ± SEM)	59 ± 15	186 ± 11	$P < 0.0001^c$

^at-test for age.^bFisher's Exact Test for elastosis score.^cMann–Whitney for p53 and COX-2 scores.**Table 3** Multivariate analysis of the association between fibroblasts, mast cells, and epithelial p53 and COX-2 expression

	Papillary mast cells ^a (P-value)	Reticular mast cells ^a (P-value)	p53 ^a (P-value)	COX-2 ^a (P-value)
Papillary fibroblasts ^b	0.042	< 0.0001	0.019	0.018
Reticular fibroblasts ^b	0.004	< 0.0001	0.068	0.310

^aPredictive variable.^bDependent variable.

and reticular areas of the lamina propria. Fibroblast density was associated with tryptase-positive mast cells and epithelial p53 and COX-2 expression. Fibroblasts also were elevated in samples with high scores of actinic elastosis, suggesting that they are important effector cells of actinic damage during early lip carcinogenesis.

Increased fibroblast density has been described previously during the formation of a reactive stroma in several neoplasias, including intraoral cancer and skin (21, 23, 28). On the other hand, *in vitro* studies have shown that UVB- and UVA-irradiated fibroblasts have reduced proliferation and increased expression of senescence and apoptotic markers (32, 33). The present results showed that fibroblasts and mast cells were increased in photodamaged lips, with an association between the density of both cell types. Similar findings were reported by Coussens et al. (28) during the early stages of skin carcinogenesis in an HPV-16 transgenic mouse model, where fibroblasts and mast cells were increased in epithelial dysplasias. In that model, mast cell-derived tryptase was considered the main mediator stimulating fibroblast proliferation (28). Several mast cell mediators, including histamine, IL-4, and tryptase, modulate fibroblast proliferation and could explain the increased fibroblast density in photodamaged lips (25, 34, 35). Specifically, tryptase increases fibroblast proliferation by activating the protease-activated receptor (PAR)-2 (35, 36), which is expressed in normal and photodamaged tissues by keratinocytes and stromal cells (6, 37–39). Therefore, mast cell-derived tryptase may be an important mediator of fibroblast activation and proliferation during early lip carcinogenesis.

An association between mast cell density and actinic elastosis has been described in photodamaged skin (12, 15, 40, 41). In the lip, a study by Costa et al. (9) found no significant association between mast cells and elastosis at the subepithelial areas or tumor front of AC and lip

squamous cell carcinoma samples, respectively. Similarly, in the present study, reticular but not papillary mast cell density was significantly increased in lip samples with high elastosis scores. On the other hand, papillary and reticular fibroblasts were elevated in lip samples with high elastosis scores, suggesting a more prominent role of fibroblasts in the pathogenesis of elastosis in photodamaged lips. Fibroblasts can stimulate solar elastosis by different mechanisms, including increased elastin and elastase production as well as matrix metalloproteinase (MMP)-1 and -2 secretion (14, 18, 19, 42, 43). In addition, the production of elastase-inducible cytokines, such as IL-8, by photodamaged keratinocytes also contributes to elastin fiber degradation by fibroblasts (14). Future studies should assess the role of these different pathways in elastosis formation in the lips.

A potent interaction between fibroblasts and keratinocytes has been shown *in vitro* and *in vivo* (24, 27, 30, 44). In this study, papillary fibroblast density also was associated with epithelial expression of COX-2 and p53. It has been demonstrated that UVB light directly stimulates keratinocyte expression of COX-2 and p53 (45). Photodamaged keratinocytes are more resistant to apoptosis and secrete growth factors (e.g., TGF- β isoforms) as well as pro-inflammatory cytokines (e.g., IL-1) that activate the stromal microenvironment, thus favoring increased fibroblast density and MMP secretion (42, 46). The results suggest that fibroblast density and activation during early lip carcinogenesis are regulated by stromal signals provided by mast cells, in addition to growth factors and cytokines secreted by photodamaged keratinocytes.

In conclusion, AC lesions have a complex stromal microenvironment characterized by increased density of fibroblasts and mast cells that are associated with ECM degradation and elastosis formation. In addition,

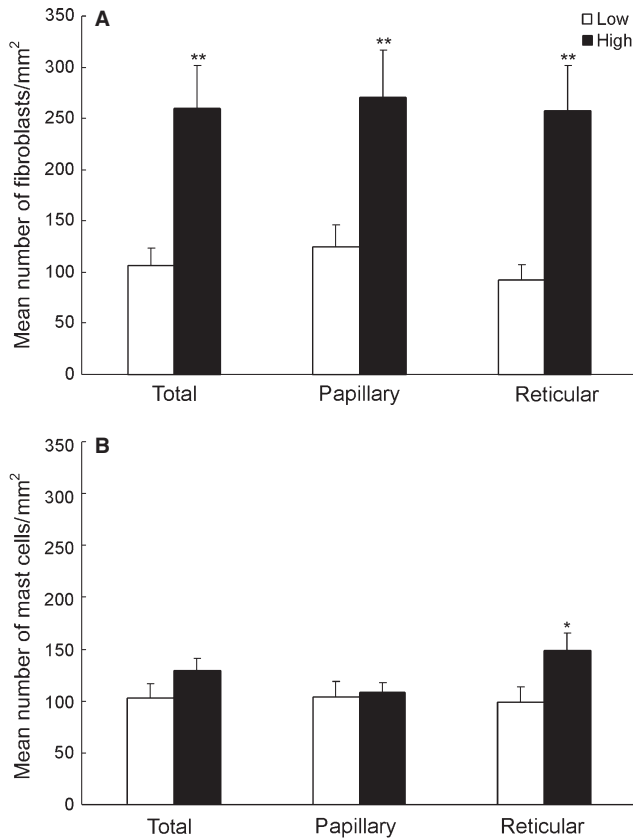


Figure 3 Association between actinic elastosis and the density of fibroblasts and mast cells. Samples were processed for elastosis detection with Verhoeff-Van Gieson stain, and elastosis scores were obtained. According to their scores, normal lip (NL) and actinic cheilitis (AC) samples were distributed into high (3–4) and low (1–2) elastosis groups and associated with the density of fibroblasts (A) and mast cells (B). Results are expressed as Mean ± SEM. ** $P < 0.01$ (t -test) for fibroblast density in total, papillary, and reticular areas of the high elastosis group as compared to the low elastosis group. * $P < 0.05$ for mast cell density in reticular areas of the high elastosis group as compared to the low elastosis group.

photodamaged keratinocytes may also contribute to stromal activation by modulating fibroblast function and proliferation. Therefore, fibroblasts may be important effector cells of actinic damage in the lip. Their function should be further characterized to determine their biological significance and their potential role as diagnostic markers of lip photodamage.

References

- Picascia DD, Robinson JK. Actinic cheilitis: a review of the etiology, differential diagnosis, and treatment. *J Am Acad Dermatol* 1987; **17**: 255–64.
- Kaugars GE, Pillion T, Svirsky JA, Page DG, Burns JC, Abbey LM. Actinic cheilitis: a review of 152 cases. *Oral Surg Oral Med Oral Pathol Oral Radiol Endod* 1999; **88**: 181–6.
- van der Waal I. Potentially malignant disorders of the oral and oropharyngeal mucosa; terminology, classification and present concepts of management. *Oral Oncol* 2009; **45**: 317–23.
- Martínez A, Brethauer U, Borlando J, Spencer ML, Rojas IG. Epithelial expression of p53, mdm-2 and p21 in

- normal lip and actinic cheilitis. *Oral Oncol* 2008; **44**: 878–83.
- Neto Pimentel DR, Michalany N, Alchorne M, Abreu M, Borra RC, Weckx L. Actinic cheilitis: histopathology and p53. *J Cutan Pathol* 2006; **33**: 539–44.
- Rojas IG, Martínez A, Brethauer U, et al. Actinic cheilitis: epithelial expression of COX-2 and its association with mast cell tryptase and PAR-2. *Oral Oncol* 2009; **45**: 284–90.
- Rojas IG, Martínez A, Pineda A, Spencer ML, Jiménez M, Rudolph MI. Increased mast cell density and protease content in actinic cheilitis. *J Oral Pathol Med* 2004; **33**: 567–73.
- Zancope E, Costa NL, Junqueira-Kipnis AP, et al. Differential infiltration of CD8+ and NK cells in lip and oral cavity squamous cell carcinoma. *J Oral Pathol Med* 2010; **39**: 162–7.
- Costa NL, Oton-Leite AF, Cheim-Júnior AP, et al. Density and migration of mast cells in lip squamous cell carcinoma and actinic cheilitis. *Histol Histopathol* 2009; **24**: 457–65.
- Berneburg M, Plettenberg H, Krutmann J. Photoaging of human skin. *Photodermatol Photoimmunol Photomed* 2000; **16**: 239–44.
- Yaar M, Gilchrist BA. Photoaging: mechanism, prevention and therapy. *Br J Dermatol* 2007; **157**: 874–87.
- Grimbaldeston MA, Finlay-Jones JJ, Hart PH. Mast cells in photodamaged skin: what is their role in skin cancer? *Photochem Photobiol Sci* 2006; **5**: 177–83.
- Gonzalez S, Moran M, Kochevar IE. Chronic photodamage in skin of mast cell-deficient mice. *Photochem Photobiol* 1999; **70**: 248–53.
- Imokawa G. Recent advances in characterizing biological mechanisms underlying UV-induced wrinkles: a pivotal role of fibroblast-derived elastase. *Arch Dermatol Res* 2008; **300**(Suppl 1): S7–20.
- Iddamalagoda A, Le QT, Ito K, Tanaka K, Kojima H, Kido H. Mast cell tryptase and photoaging: possible involvement in the degradation of extra cellular matrix and basement membrane proteins. *Arch Dermatol Res* 2008; **300**(Suppl 1): S69–76.
- Bhawan J, Andersen W, Lee J, Labadie R, Solares G. Photoaging versus intrinsic aging: a morphologic assessment of facial skin. *J Cutan Pathol* 1995; **22**: 154–9.
- Sorrell JM, Caplan AI. Fibroblast heterogeneity: more than skin deep. *J Cell Sci* 2004; **117**: 667–75.
- Tsukahara K, Takema Y, Moriwaki S, et al. Selective inhibition of skin fibroblast elastase elicits a concentration-dependent prevention of ultraviolet B-induced wrinkle formation. *J Invest Dermatol* 2001; **117**: 671–7.
- Codriansky KA, Quintanilla-Dieck MJ, Gan S, Keady M, Bhawan J, Rüniger TM. Intracellular degradation of elastin by cathepsin K in skin fibroblasts—a possible role in photoaging. *Photochem Photobiol* 2009; **85**: 1356–63.
- Martin P. Wound healing—aiming for perfect skin regeneration. *Science* 1997; **276**: 75–81.
- Kalluri R, Zeisberg M. Fibroblasts in cancer. *Nat Rev Cancer* 2006; **6**: 392–401.
- Wynn TA. Cellular and molecular mechanisms of fibrosis. *J Pathol* 2008; **214**: 199–210.
- Thode C, Jørgensen TG, Dabelsteen E, Mackenzie I, Dabelsteen S. Significance of myofibroblasts in oral squamous cell carcinoma. *J Oral Pathol Med* 2011; **40**: 201–7.
- Tuan TL, Keller LC, Sun D, Nimni ME, Cheung D. Dermal fibroblasts activate keratinocyte outgrowth on collagen gels. *J Cell Sci* 1994; **107**: 2285–9.

25. Trautmann A, Krohne G, Bröcker EB, Klein CE. Human mast cells augment fibroblast proliferation by heterotypic cell-cell adhesion and action of IL-4. *J Immunol* 1998; **160**: 5053–7.
26. Krtolica A, Parrinello S, Lockett S, Desprez PY, Campisi J. Senescent fibroblasts promote epithelial cell growth and tumorigenesis: a link between cancer and aging. *Proc Natl Acad Sci USA* 2001; **98**: 12072–7.
27. Bhowmick NA, Neilson EG, Moses HL. Stromal fibroblasts in cancer initiation and progression. *Nature* 2004; **432**: 332–7.
28. Coussens LM, Raymond WW, Bergers G. Inflammatory mast cells upregulate angiogenesis during squamous epithelial carcinogenesis. *Genes Dev* 1999; **13**: 1382–97.
29. Artuc M, Steckelings UM, Henz BM. Mast cell-fibroblast interactions: human mast cells as source and inducers of fibroblast and epithelial growth factors. *J Invest Dermatol* 2002; **118**: 391–5.
30. Mueller MM, Fusenig NE. Friends or foes – bipolar effects of the tumour stroma in cancer. *Nat Rev Cancer* 2004; **4**: 839–49.
31. Schütz A, Tannapfel A, Wittekind C. Comparison of different double immunostaining protocols for paraffin embedded liver tissue. *Anal Cell Pathol* 1999; **18**: 227–33.
32. Straface E, Vona R, Ascione B, et al. Single exposure of human fibroblasts (WI-38) to a sub-cytotoxic dose of UVB induces premature senescence. *FEBS Lett* 2007; **581**: 4342–8.
33. Chainiaux F, Magalhaes JP, Eliaers F, Remacle J, Toussaint O. UVB-induced premature senescence of human diploid skin fibroblasts. *Int J Biochem Cell Biol* 2002; **34**: 1331–9.
34. Garbuzenko E, Nagler A, Pickholtz D, et al. Human mast cells stimulate fibroblast proliferation, collagen synthesis and lattice contraction: a direct role for mast cells in skin fibrosis. *Clin Exp Allergy* 2002; **32**: 237–46.
35. Frungieri MB, Weidinger S, Meineke V, Köhn FM, Mayerhofer A. Proliferative action of mast-cell tryptase is mediated by PAR2, COX2, prostaglandins, and PPAR-gamma: possible relevance to human fibrotic disorders. *Proc Natl Acad Sci USA* 2002; **99**: 15072–7.
36. Shpacovitch V, Feld M, Hollenberg MD, Luger TA, Steinhoff M. Role of protease-activated receptors in inflammatory responses, innate and adaptive immunity. *J Leukoc Biol* 2008; **83**: 1309–22.
37. D'Andrea MR, Derian CK, Leturcq D, et al. Characterization of protease-activated receptor-2 immunoreactivity in normal human tissues. *J Histochem Cytochem* 1998; **46**: 157–64.
38. Scott G, Deng A, Rodriguez-Burford C, et al. Protease-activated receptor 2, a receptor involved in melanosome transfer, is upregulated in human skin by ultraviolet irradiation. *J Invest Dermatol* 2001; **117**: 1412–20.
39. Steinhoff M, Corvera CU, Thoma MS, et al. Proteinase-activated receptor-2 in human skin: tissue distribution and activation of keratinocytes by mast cell tryptase. *Exp Dermatol* 1999; **8**: 282–94.
40. Lavker RM, Kligman AM. Chronic heliodermatitis: a morphologic evaluation of chronic actinic dermal damage with emphasis on the role of mast cells. *J Invest Dermatol* 1988; **90**: 325–30.
41. Hernández-Barrera R, Torres-Alvarez B, Castanedo-Cazares JP, Oros-Ovalle C, Moncada B. Solar elastosis and presence of mast cells as key features in the pathogenesis of melasma. *Clin Exp Dermatol* 2008; **33**: 305–8.
42. Wang XY, Bi ZG. UVB-irradiated human keratinocytes and interleukin-1 α indirectly increase MAP kinase/AP-1 activation and MMP-1 production in UVA-irradiated dermal fibroblasts. *Chin Med J* 2006; **119**: 827–31.
43. Ohnishi Y, Tajima S, Akiyama M, Ishibashi A, Kobayashi R. Expression of elastin-related proteins and matrix metalloproteinases in actinic elastosis of sun-damage skin. *Arch Dermatol Res* 2000; **292**: 27–31.
44. Singer AJ, Clark RA. Cutaneous wound healing. *N Engl J Med* 1999; **341**: 738–46.
45. Bowden GT. Prevention of non-melanoma skin cancer by targeting ultraviolet-B-light signalling. *Nat Rev Cancer* 2004; **4**: 23–35.
46. Gold LI, Jussila T, Fusenig NE, Stenbäck F. TGF- β isoforms are differentially expressed in increasing malignant grades of HaCaT keratinocytes, suggesting separate roles in skin carcinogenesis. *J Pathol* 2000; **190**: 579–88.

Acknowledgements

This research was supported by the Chilean Council for Science and Technology CONICYT, grants FONDECYT 1090287 and 1050581. The authors also wish to thank Mr Brian Freeburg and Ms Amanda Harper for proofreading this manuscript.

Conflict of interest

None declared.